Compatibilization of Poly(2,6-dimethyl-1,4-phenylene oxide)/Polyamide 6 Blends with Styrene–Maleic Anhydride Copolymer: Mechanical Properties, Morphology, Crystallization, and Melting Behavior

Shuai Wang, Bo Li, Yong Zhang

The State Key laboratory of Metal Matrix Composites, School of Chemistry and Chemical Engineering, Shanghai Jiao Tong University, Shanghai 200240, China

Received 19 January 2009; accepted 26 April 2010
DOI 10.1002/app.32730
Published online 14 July 2010 in Wiley InterScience (www.interscience.wiley.com).

ABSTRACT: Styrene–maleic anhydride copolymer (SMA) with higher MA content (21.8 wt %) than reported SMA (mostly 8 wt %) was used as a compatibilizer for poly(2,6-dimethyl-1,4-phenylene oxide) (PPO)/polyamide 6 (PA6) blends by *in situ* formed PA-*g*-SMA during melt processing. The tensile strength and flexural strength of PPO/PA blends were greatly increased by the addition of SMA. The morphology of PPO/PA/SMA (30/70/variable) was investigated by scanning electron microscopy, and the addition of SMA led to a significant decrease in the particle size of the dispersed PPO phase. Melting and crystallization of PPO/PA/SMA blends were studied by differential scanning calorimetry, and the results showed that the addition of SMA could improve the compatibility between PPO and PA. The *in situ* reaction between PA and SMA was confirmed by Fourier transform infrared analysis. SMA was an effective compatibilizer for PPO/PA blends, and its compatibilization mechanism was discussed. © 2010 Wiley Periodicals, Inc. J Appl Polym Sci 118: 3545–3551, 2010

Key words: PPO; PA; compatibilization; SMA

INTRODUCTION

Poly(2,6-dimethyl-1,4-phenylene oxide) (PPO) has high tensile strength, good dimensional stability, good water resistance, and high glass-transition temperature, but it also possesses low melt flow ability and poor processability, natural brittleness, and poor solvent resistance.[1–3] Polyamide 6 (PA6) has good melt flow ability and excellent solvent resistance with deficiencies like poor water resistance, poor heat resistance, and low dimensional stability.[4–6] PPO and PA6 are expected to be melt mixed together to achieve blends that could keep their good properties and compensate the individual deficiencies. A key problem of PPO/PA blends is the immiscibility of PPO and PA, so compatibilization is usually needed.

Compared to copolymerization or graft polymerization,[7,8] which was considered as an effective method to compatibilize PPO/PA blends, the addition of compatibilizers should be a more convenient and costless way to apply to the industry. Functionalized PPO was another useful method to compatibilize PPO/PA blends during the mixing procedure.[2,9] Maleic anhydride-grafted PPO (PPO-*g*-MA) was used as a reactive compatibilizer in polystyrene(PS)/PPO/PA6 blends, in which PS was located in PPO phase because of their intrinsic miscibility.[10] The addition of PPO-*g*-MA reduced the flow-induced deformation, the coalescence and the breakup of particles in injection molding process, yielding a more uniform morphology.[10,11]

Styrene–maleic anhydride copolymer (SMA) was often used to compatibilize PPO/PA blends because it has segments which are miscible with PPO and maleic anhydride (MA) which could react with PA.[12] Chiang and Chang[13] used SMA with 8 wt % of MA to compatibilize PPO/PA blends and achieved good mechanical properties by *in situ* reactions. Dedecker and Groeninckk[5] also used SMA (8 wt % MA) as a compatibilizer for PPO/PA and studied the reactions between PA6 and SMA. Chu et al.[14] studied the correlation between the molecular dynamics and mechanical properties of PPO/PA compatibilized by SMA (8 wt % MA). The addition of SMA reduced the size of dispersed phase (PA)

Correspondence to: Y. Zhang (yong_zhang@sjtu.edu.cn).
Contract grant sponsor: Special Funds of Technological Cooperation between Qingpu District (Shanghai) and Shanghai Jiao Tong University.
Contract grant sponsor: Funds of Science and Technology Commission of Shanghai Municipality; contract grant number: 06XD14213.
Contract grant sponsor: Shanghai Leading Academic Discipline Project; contract grant number: B202.

and increased the interfacial contact area, leading to the increase in the tensile strength and unnotched impact strength.[14]

SMA with 8 wt % MA was considered as the proper compatibilizer for PPO and PA, compared to the SMA with lower content of MA, such as SMA with 2 wt % MA.[5] However, SMA with such a high content of MA (21.8 wt %) as the compatibilizer for PPO/PA blends has not been reported so far. In this article, this kind of SMA was selected as a reactive compatibilizer. SMA with less than 8% of MA was considered to be miscible with PPO and majorly distributed in PPO phase,[5] but SMA with 21.8% MA used in this article may prefer to be located in the interface between PPO and PA because of its high polarity, which may reduce the interfacial energy and suppress coalescence of PPO/PA blends.

The effect of SMA (21.8 wt % MA) on the mechanical properties, morphology, crystallization, and melting behavior of PPO/PA blends was also discussed.

EXPERIMENTAL

Materials

PPO, Iupiace PX100L, produced by Asahi Kasei Corporation, has an intrinsic viscosity of 0.47 ± 0.02 dL/g measured in chloroform at 25°C. PA6, provided by Kingfa Sci & Tech. Co., LTD., has a relative viscosity of 2.4. SMA, Xiran SZ22065, produced by Polyscope Polymers, the Netherlands, has an intrinsic viscosity of 0.327 dL/g measured in tetrahydrofuran (THF) and the MA content of 21.8 wt % measured by near infrared spectroscopy.

Sample preparation

PPO, PA6, and SMA were dried at 80°C under vacuum for 12 h and premixed for 5 min before extrusion. The mixture was extruded in a co-rotating twin-screw extruder (L/D = 41, D = 25 mm) at a processing temperature range of 230–250°C and a rotation speed of 200 rpm.

The extruded blend was dried in a vacuum oven at 80°C for 12 h before injection molding. The barrel temperature was 255/255/250/250/240°C and the mold temperature was 80°C. The injection pressure was set at 40–60 MPa, whereas the holding pressure was set at 30–50 MPa. The holding time and cooling time were 10 s and 20 s, respectively.

Measurements

Tensile and flexural properties were measured using an Instron 4465 universal testing instrument (Instron, USA) according to ASTM D638 and D790. The dumbbell shaped specimens were tested at a crosshead speed of 50 mm/min for tensile test at 23°C. Flexural properties were measured using 63.5 × 12.7 × 3.2 mm^3 specimens at a crosshead speed of 1.7 mm/min at 23°C.

Notched Izod impact strength was measured using 63.5 × 12.7 × 3.2 mm^3 specimens with a V-shape notch on a Ray-Ran universal pendulum impact tester according to ASTM D256. The hammer speed was 3.5 m/s and the pendulum weight was 0.818 kg.

The morphology of fracture surfaces of specimens was studied using field emission scanning electron microscope (FESEM, JSM-7401F, JEOL, Japan). The fracture surfaces were etched with chloroform for 6 h at room temperature to selectively dissolve PPO. The etched samples were kept in vacuum for 8 h at 80°C to remove chloroform and then sputter-coated with a thin gold layer before observation.

The number-average diameter of the domains, which represented the dispersed phase (PPO), was determined according to the following equation:

$$D_n = \sum N_i D_i / \sum N_i \quad (1)$$

where N_i is the number of PPO domains with the diameter of D_i, and the total number of domains taken into account is about 200–250.

Melting behavior of PPO/PA/SMA blends was investigated by differential scanning calorimeter (DSC, Pyris 1, Perkin Elmer, USA). The samples were first heated from 0 to 300°C at 50°C/min under a nitrogen atmosphere and held for 3 min at 300°C, then cooled to 0°C at 20°C/min, and reheated to 300°C at 20°C/min. The second heating DSC curves were recorded to characterize the melting behavior and crystallization ability.

The X-ray diffraction patterns were recorded using D/max-2200/PC (Rigaku Co., Japan). The scanning rate was 5°/min and the angle range was from 5° to 40°. The samples with size of 10 × 10 × 1 mm^3 were first heated from 0 to 300°C at 50°C/min under a nitrogen atmosphere and held for 3 min at 300°C, then cooled to 0°C at 20°C/min, and reheated to 300°C at 20°C/min.

The films of PPO, PA, SMA, and PPO/PA/SMA (30/70/10) about 100 μm thick were obtained by compression moulding at 250°C and characterized by a Fourier transform infrared spectrometer (FTIR, Paragon 1000, Perkin Elmer, USA).

Melt viscosity was measured at 260°C using an Instron 4467 capillary rheometer (Instron, USA) with the die length/diameter ratio (L/D) of 40/1 and an entrance angle of 180°. The Rabinowitch and Bagley corrections were applied to all the experimental data.

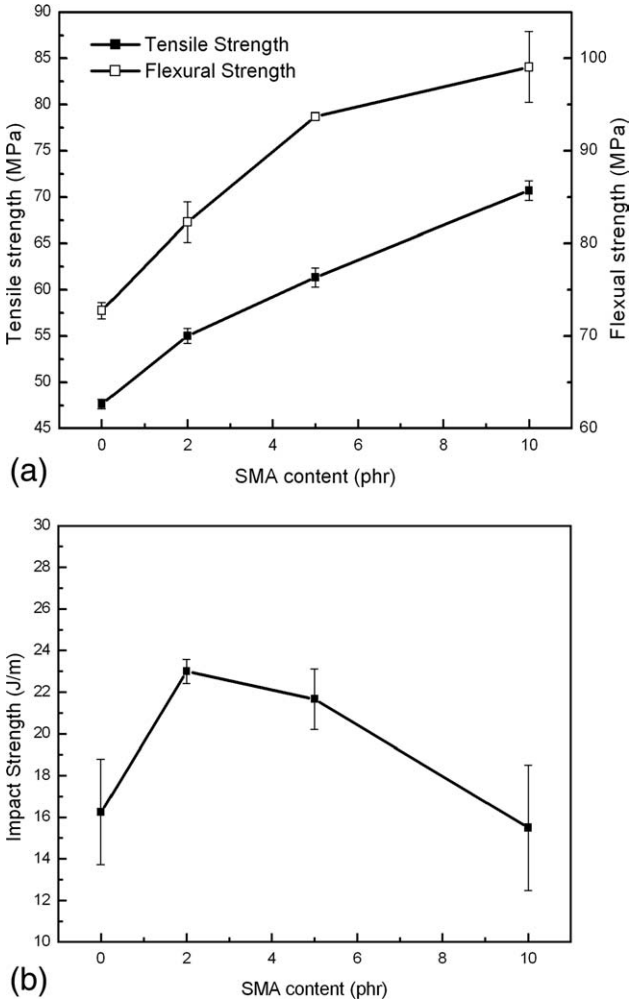

Figure 1 Mechanical properties of PPO/PA6/SMA blends: (a) tensile and flexural strength; (b) notched Izod impact strength.

RESULTS AND DISCUSSION

Mechanical properties

PPO is a brittle material. Tensile and flexural strengths of PPO/PA6/SMA blends are shown in Figure 1(a). The addition of SMA into PPO/PA6 (30/70) blend had a great effect on the mechanical properties of the blend. The tensile and flexural strength increased drastically with increasing SMA content. For PPO/PA (30/70), the tensile strength increased drastically from 47.6 to 70.7 MPa when 10 phr SMA was added. But in Chiang's work,[13] the tensile strength of the PPO/PA (30/70) increased from 29 to 44 MPa after the same content of SMA (8 wt % MA) was added. The difference might be due to two reasons: (1) the higher content of MA would lead to the higher degree of chain extension of PA molecules and accordingly the higher melting viscosity of PA6 component match more that of PPO component, resulting in a better compatibility as well as better mechanical properties of the blends; (2) the higher content of MA would facilitate the dispersion of SMA as a compatibilizer both in PA6 phase and PPO phase, thus improving the compatibilization effect on incompatible PPO/PA blends and resulting in a higher tensile strength.

The notched Izod impact strength of PPO/PA was 16.3 J/m and increased to 23.0 J/m with the addition of SMA (2 phr), which was 1.42 times of that of PPO/PA. Further increasing SMA content led to a decrease of the notched Izod impact strength. Chiang and Chang[13] found the unnotched Izod impact strength increased with increasing SMA (8 wt %) content. The decrease of notched Izod impact strength at high content of SMA (over 2 phr) might be attributed to the excessive content of SMA. The SMA used in this study has higher MA content than the commonly used commercial SMA, so the proper content of SMA to compatibilize PPO/PA should not be so much as those in the other researchers' results.

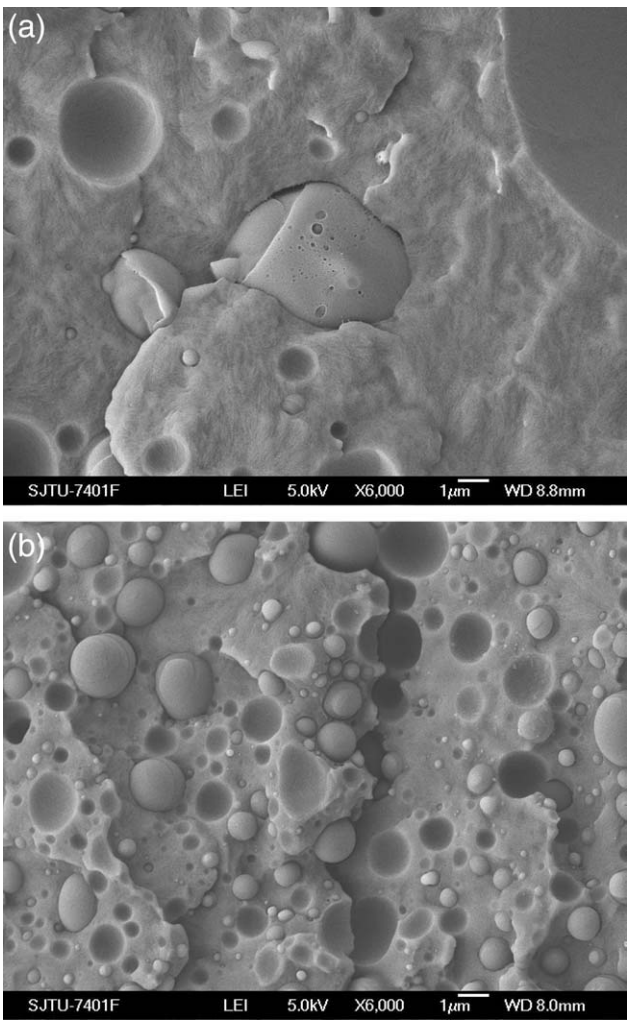

Figure 2 SEM microphotos of PPO/PA/SMA blends: (a) PPO/PA (30/70), (b) PPO/PA/SMA (30/70/10).

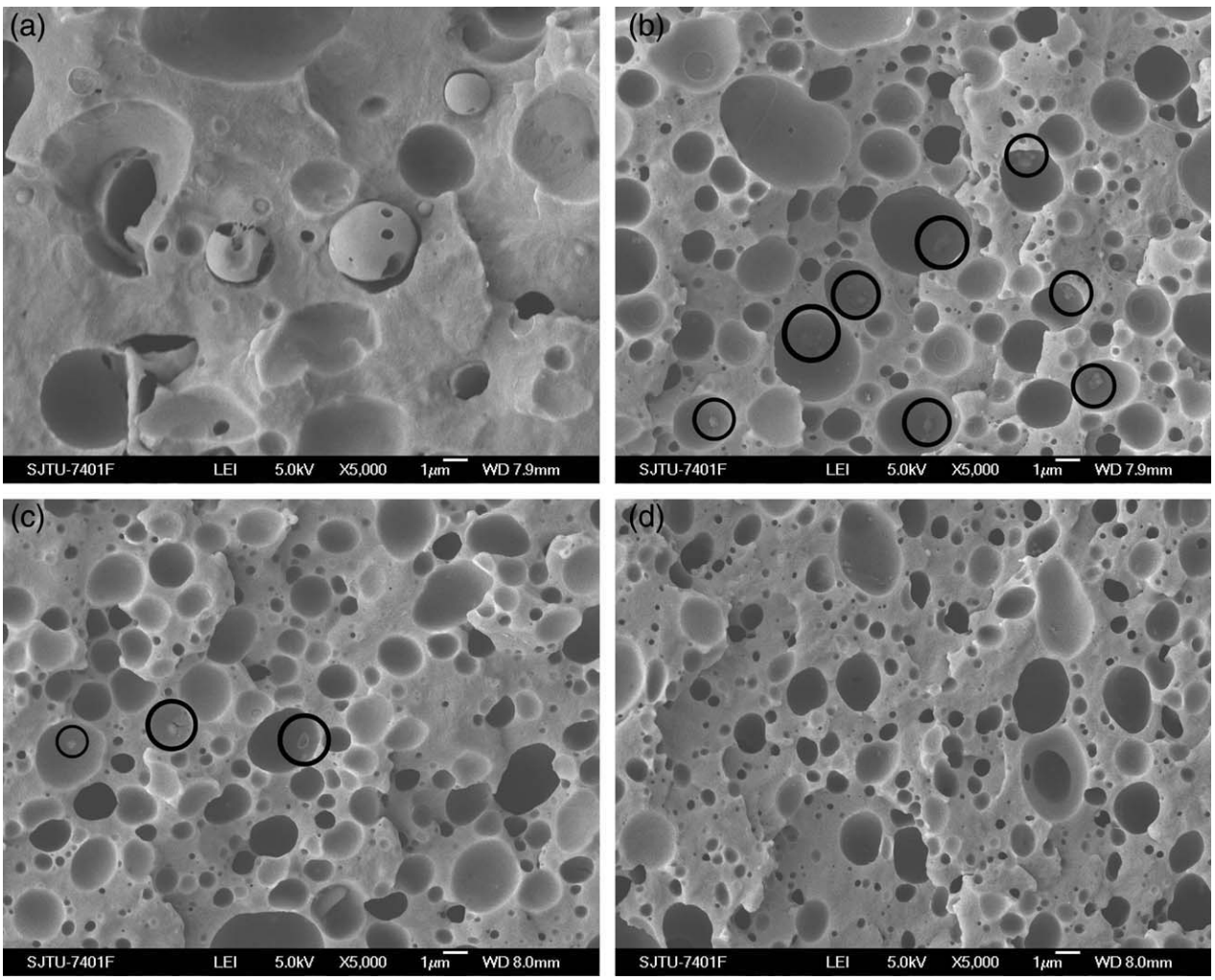

Figure 3 SEM microphotos of PPO/PA/SMA blends etched by chloroform: (a) PPO/PA (30/70), (b) PPO/PA/SMA (30/70/2), (c) PPO/PA/SMA (30/70/5), (d) PPO/PA/SMA (30/70/10).

Morphology

Phase size and morphology of polymer blends are always used to illustrate the compatibilization effect. SEM microphotos of PPO/PA/SMA fracture surfaces are shown in Figure 2. The cavities in the pictures represented for PPO which was pulled out when fracture happened, considering that PPO accounted for about 30 wt % in the blends and PA has a lower viscosity which made it the continuous phase. It is clear that PPO was dispersed in PA phase unevenly in Figure 2(a), while the size of dispersed phase decreased significantly and the small PPO particles dispersed more uniformly in PA6 phase after the addition of SMA in Figure 2(b). It is consistent with the preceding analysis: the presence of SMA in the PPO/PA blend improved the compatibility between PPO and PA and thus improved the mechanical properties of the blend.

SEM microphotos of the etched fracture surface of PPO/PA blends by chloroform are shown in Figure 3. Chloroform is a good solvent for PPO but a nonsolvent for PA. So the cavities were observed after dissolving PPO, and PA was left behind as the continuous phase. As seen in Figure 3(a), the cavities were not uniformly dispersed and had large size. In Figure 3(b,c), there were small granules dispersed on the cavities which represented the residue of SMA, as marked with black circles. And the interface was much fuzzier, especially in Figure 3(b), compared to the interface observed in the other photos. In a word, 2 or 5 phr SMA had better compatibilizing effect on PPO/PA than the higher SMA content for the overall analysis.

The size of the dispersed phase was calculated using software called MiVnt. More than two hundred of dispersed domains were counted to calculate the average size of the dispersed phase to imply the compatibility between PPO and PA. The statistical curves depicting the equivalent diameters of the dispersed phase of the blends are shown in Figure 4.

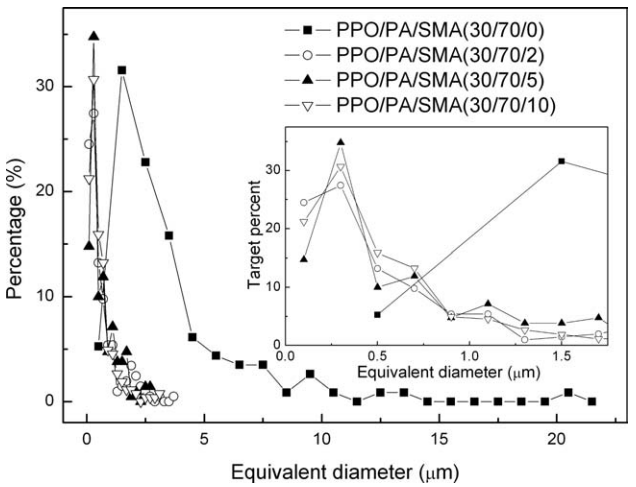

Figure 4 Statistical graph of the dispersed phase of PPO/PA/SMA blends.

The sizes of the dispersed phase in PPO/PA without SMA were not uniform and spread from 0.1 to 21.5 μm. However, the addition of SMA led to great changes. Most of the dots assembled together, which meant the sizes of cavities were in the same scale (from 0.1 to 4.0 μm).

The average diameter of the dispersed phase was 3.42 μm for PPO/PA blend, while the equivalent diameters of PPO for PPO/PA/SMA blends with SMA content of 2 phr, 5 phr, and 10 phr were 0.64, 0.67, and 0.56 μm, respectively. The standard deviation of the equivalent diameter of PPO/PA (30/70) was 2.97, while the others were 0.66, 0.58, and 0.51, which meant that the size of dispersed phase was more uniform with the addition of SMA, indicating the improvement of compatibility between PPO and PA.

Crystallization and melting behavior

DSC was used to investigate the melting behavior of PPO/PA/SMA. The glass transition temperatures (T_g) of PPO and PA could be used to investigate the compatibility of PPO and PA. As shown in Figure 5(a) and Table I, T_g of PPO is 219.0°C and T_g of PA is 50.0°C, while T_g of PA component in PPO/PA (30/70) blend is 51.4°C. With increasing SMA content, the

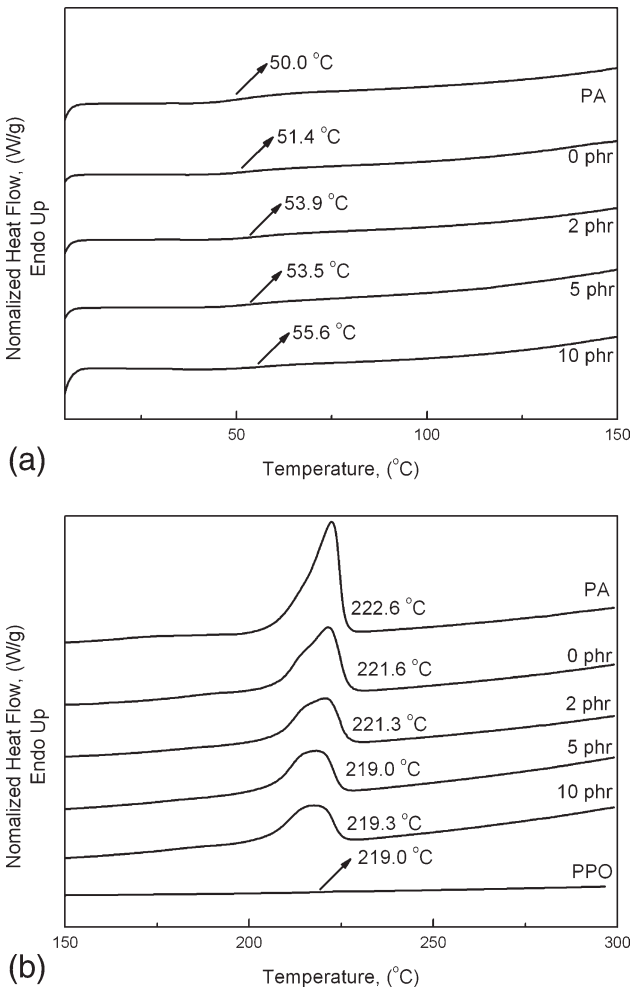

Figure 5 The heating curves of PPO, PA, and PPO/PA/SMA (30/70/variable) blends by DSC: (a) T_g of PA; (b) T_m of PA.

glass transition temperature of PA shifted to higher temperature by nearly 4.2°C at the SMA content of 10 phr, which might be due to the compatibilization effect of SMA on incompatible PPO/PA (30/70) blends.

The melting peak of PPO could hardly be observed in the second heating curve, so the melting peaks in the second heating curves in Figure 5(b) represented the melting temperatures (T_m) for PA. As seen in Table I, the addition of SMA led to a slight decrease of T_m of PA. As mentioned before,

TABLE I
Thermal Analysis Parameters of PPO, PA, and PPO/PA/SMA (30/70/variable) Blends

PPO/PA/SMA (phr)	$T_{g,PA}$ (°C)	$T_{m,PA}$ (°C)	ΔH_f (J/g)	$X_{C,PA}$ (%)
100/0/0	–	–	–	–
0/100/0	50.0	222.6	49.8	–
30/70/0	51.4	221.6	30.1	18.7
30/70/2	53.9	221.3	24.3	15.4
30/70/5	53.5	219.0	23.9	15.6
30/70/10	55.6	219.3	21.6	14.8

SMA might react with PA, so the original linear structure of PA molecular chains was changed and the regular piling of chains was also influenced. Consequently, the melting peak shifted to a lower temperature.

The crystallinity of a polymer usually has a great effect on its mechanical properties.[15] The crystallinity of PPO was 0 in the second heating scan as shown in Figure 5, so the heat enthalpy in the curves represented for PA. The crystallinity of PA phase could be obtained by the following equation:

$$X_{C,PA} = \frac{\Delta H_f}{\Delta H_0 \times W_{PA}} \times 100 \quad (2)$$

where $X_{C,PA}$ is the crystallinity of PA, ΔH_0 is the thermodynamic enthalpy of fusion per gram of PA (230 ± 20 J/g),[16] ΔH_f is the apparent enthalpy of fusion per gram of the blends; W_{PA} is the weight content of PA. Although PA has three types of crystals, α, β and γ, the other two kinds of crystals would almost transform to α crystals during the heating run. So the thermodynamic enthalpy of fusion per gram of PA represents for α crystals.[17] Wide angle X-ray diffraction patterns of PA after the same heating treatment as DSC are shown in Figure 6, where the two peaks, [200] and [002]/[202] represented for the characterized peaks of α phase of PA 6. And the melting temperature near 220°C further proved α phase of PA 6.

As shown in Table I, the crystallinity decreased significantly with increasing SMA content, indicating that SMA had a negative effect on the crystallization of PA.

FTIR analysis

The FTIR spectra of PPO/PA6/SMA blends with different SMA content are shown in Figure 7. The bands at 1856 and 1780 cm^{-1} were emerging with the increasing content of SMA, and the bands around 1500 cm^{-1} were becoming less sharp and merged together. The FTIR result of PPO/PA6/SMA (30/70/10) was selected to compare with the FTIR result of PPO, PA6, and SMA to further understand the compatibilization mechanism.

Figure 8 shows the FTIR spectra of PPO, PA, SMA, and PPO/PA/SMA (30/70/10) blend. The characteristic absorption bands of SMA at 1858 and 1772 cm^{-1} are the carbonyl resonance by the MA group,[13] as shown in Figure 7. The ring stretching of styrene occurs at the absorption band of 1602 cm^{-1}. $\nu_{C=O}$ stretching and ν_{N-H} bending of PA6 are near 1644 cm^{-1}. However, most of the bands were shielded because of the addition of PPO.

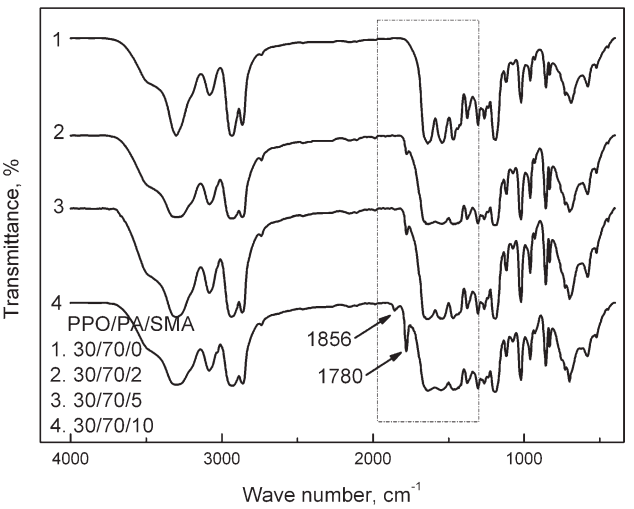

Figure 7 FTIR data of PPO/PA/SMA (30/70/variable) blends.

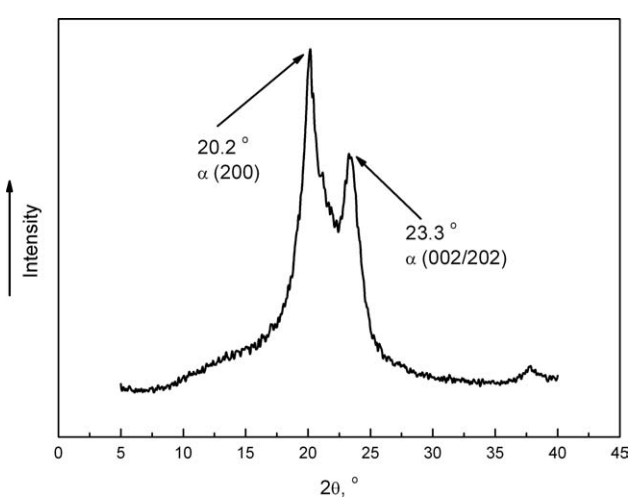

Figure 6 Wide angle X-ray diffraction pattern of PA after heating treatment.

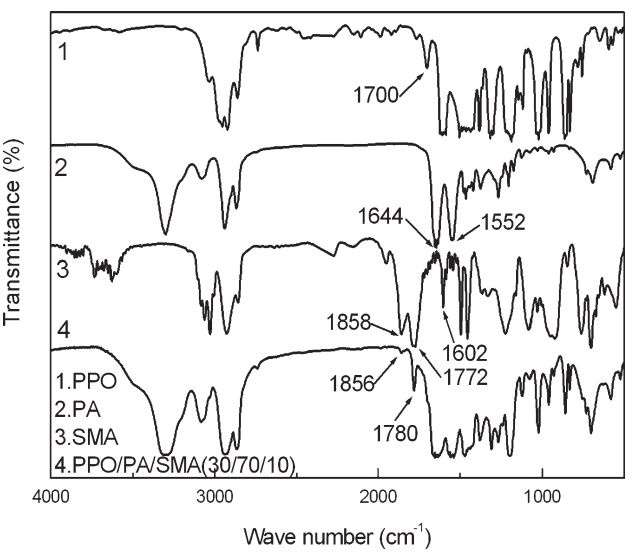

Figure 8 FTIR data of PPO, PA, SMA, and PPO/PA/SMA (30/70/10) blend.

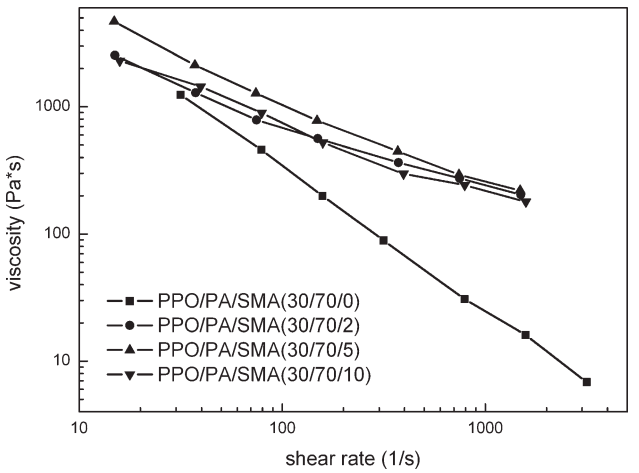

Figure 9 Capillary rheological curves for the PPO/PA6/SMA (30/70/variable) blends.

It was obvious that the characteristic absorption bands for SMA near 1856 and 1780 cm^{-1} changed greatly because of the addition of SMA in the blend, comparing to FTIR spectrum of SMA in Figure 8. However, they did not shrink at the same ratio. The peak at 1856 cm^{-1} could hardly be observed in the FTIR spectrum for the blend. It was presumed that the two peaks would decrease at the same minification if SMA was simply blended with PPO and PA without any reaction taking place. However, here different minifications were recognized, which further proved the existence of an *in situ* reactions between PA6 and SMA.

Rheological behavior

Figure 9 shows the plots of viscosity versus shear rate. All polymer blends exhibit substantially shear-thinning in the range of the shear rates investigated. The viscosity of PPO/PA blend decreased dramatically with increasing shear rate. The other three curves had relatively lower slopes. This could be attributed to two reasons: (1) with the addition of SMA, the reactions between SMA and PA took place and thus caused the increase of molecular weight and the interfacial friction; (2) unreacted or lightly reacted SMA helped plasticizing of PPO. SMA can plasticized PPO as reported before.[13] SMA with 10 phr in this study would help plasticizing PPO, so the PPO/PA/SMA (30/70/10) had lower viscosity than PPO/PA/SMA blends with 2 phr or 5 phr SMA at low shear rates.

CONCLUSIONS

SMA with high MA content (21.8 wt %) was used to compatibilize PPO/PA6 blend through an *in situ* formed PA-*g*-SMA during melt processing. The tensile and flexural strengths increased with increasing SMA content because of the improved compatibility between PPO and PA in the presence of SMA. The notched Izod impact strength of PPO/PA (30/70) increased 1.42 times after the addition of 2 phr SMA. The compatibilization effect of SMA on PPO/PA blend was confirmed by SEM and DSC analysis. The size of dispersed phase (PPO) decreased significantly, and the glass transition temperatures of PA shifted to high temperatures after the addition of SMA. The mechanism of compatibilization of PPO/PA blend by SMA was proved by FTIR and capillary rheological results, which implied the *in situ* formation of PA-*g*-SMA. SMA with MA content of 21.8% was useful for compatibilizing PPO and PA, leading to better mechanical properties of PPO/PA/SMA, especially at 2 phr or 5 phr SMA.

References

1. Jana, S. C.; Patel, N.; Dharaiya, D. Polymer 2001, 42, 8681.
2. Ji, Y.; Li, W.; Ma, J.; Liang, B. Macromol Rapid Commun 2005, 26, 116.
3. Miyata, K.; Watanabe, Y.; Itaya, T.; Tanigaki, T.; Inoue, K. Macromolecules 1996, 29, 3694.
4. Li, Y.; Xie, T.; Yang, G. J Appl Polym Sci 2006, 99, 2076.
5. Dedecker, K.; Groeninckx, G. J Appl Polym Sci 1999, 73, 889.
6. Liu, A.; Xie, T.; Yang, G. Macromol Chem Phys 2006, 207, 1174.
7. Chiang, C. R.; Chang, F. C. J Polym Sci Part B: Polym Phys 1998, 36, 1805.
8. Chao, H. S. I.; Hovatter, T. W. Polym Bull 1987, 17, 423.
9. Brown, S. B. U.S. Pat. 5,001,201 (1991).
10. Son, Y.; Ahn, K. H.; Char, K. Polym Eng Sci 2000, 40, 1385.
11. Son, Y.; Ahn, K. H.; Char, K. Polym Eng Sci 2000, 40, 1376.
12. Harrats, C.; Dedecker, K.; Groeninckx, G.; Jérôme, R. Macromol Symp 2003, 198, 183.
13. Chiang, C. R.; Chang, F. C. Polymer 1997, 38, 4807.
14. Chu, P. P.; Huang, J. M.; Wu, H. D.; Chiang, C. R.; Chang, F. C. J Polym Sci Part B: Polym Phys 1999, 37, 1155.
15. Kong, Y.; Hay, J. N. Polymer 2002, 43, 3873.
16. Khanna, Y. P.; Kuhn, W. P. J Polym Sci Part B: Polym Phys 1997, 35, 2219.
17. Penel-Pierron, L.; Depecker, C.; Seguela, R.; Lefebvre, J. M. J Polym Sci Part B: Polym Phys 2001, 39, 484.